Low-frequency $1/f$ fluctuations in hydrodynamic and magnetohydrodynamic turbulence

Pablo Dmitruk* and W. H. Matthaeus
Bartol Research Institute and Department of Physics and Astronomy, University of Delaware, Newark, Deleware 19716, USA
(Received 24 May 2007; published 12 September 2007)

We investigate the occurrence of $1/f$ spectra of low-frequency fluctuations in numerical simulations of three-dimensional hydrodynamic and magnetohydrodynamic turbulence driven by a random forcing with a controlled correlation time. A range of one decade of $1/f$ spectrum is observed when a strong background magnetic field is present. The frequency spectra of individual Fourier modes is also analyzed and it is observed that the $1/f$ range is present in the largest available wavelength mode for the magnetohydrodynamic simulations with and without a background magnetic field and it is not observed (or is less clear) for the hydrodynamic case. The presence of $1/f$ spectra of low-frequency fluctuations is also analyzed for two-dimensional magnetohydrodynamic and hydrodynamic turbulence simulations and it is observed in both cases. The origin of these long period fluctuations is discussed.

DOI: 10.1103/PhysRevE.76.036305 PACS number(s): 47.27.Gs, 47.27.ek, 52.30.Cv

I. INTRODUCTION

The appearance of so-called $1/f$ noise, or "flicker" noise in a variety of natural and nonlinear systems is widely regarded as a signature of some kind of scale invariant feature of the underlying dynamical processes. The distinctive characteristic is a spectral density $P(f)$ (the Fourier transform of the two-time autocorrelation function [1]) of the form $\sim 1/f$ for some range of frequency f. This implies equal energy per octave independent of f, for the corresponding range of frequencies. Time records having a range of $1/f$ spectral density have been reported in systems as wide ranging as electronics, tree growth, astrophysical dynamics, interplanetary magnetic fields, and human activities such as music and the stock market [2]. This widespread occurrence has motivated theoretical activity to identify robust pathways for generating this type of random fluctuation, loosely classified as "noise." Indeed, generic pathways for generating flicker noise have been found, based, for example, in systems with broad distributions of characteristic time scales [3], especially those with scale invariant properties [2] which can emerge in many systems having log-normal statistics associated with multiplicative processes [4]. The emergence of these properties in nonlinear systems has been associated with unifying principles, such as self-organized criticality [5]. Given the familiarity of the set of conditions, especially in nonlinear systems, that can give rise to $1/f$ noise, one might expect that fluid turbulence, in some sense a paradigm of nonlinear behavior, would be a prime candidate for finding this signature. As far as we are aware, however, there is no clear record of identification of flicker noise in turbulence (see, however, [6]), and no clear statements in the literature regarding the conditions, if any, in which one might expect to see $1/f$ noise in a fluid. Here we address this problem directly, by examining numerical simulations of turbulence in hydrodynamic and magnetohydrodynamic (MHD) turbulent flows as moderate Reynolds number. We find some useful working principles for deciding whether one expects to see flicker noise for a range of turbulence parameters.

Turbulence is characterized by the involvement of multiple space and time scales [7]. Nonlinearity, by way of the usual estimates, introduces a broad range of time scales. For example, the local hydrodynamic nonlinear time $\tau_{nl} = 1/(kv_k)$, in terms of wave-number mode k (length scale $l = 1/k$) and fluid velocity amplitude v_k at scale $1/k$, extends several orders of magnitude according to the amplitude $v_k = \sqrt{kE(k)}$ that is obtained from the standard Kolmogorov kinetic energy spectrum, $E(k) \sim \epsilon^{2/3} k^{-5/3}$, with steady energy transfer rate ϵ. The nonlinear time at scale $1/k$ is then $\tau_{nl} \sim (L/u)(kL)^{-2/3}$ [with L a characteristic large scale and u the root-mean-square (rms) velocity], extending from the large scale turnover time at $kL=1$ toward higher frequencies as kL becomes large in the inertial range. In this picture, there is no obvious way to generate correlated signals at frequencies much lower than u/L.

MHD nonlinear time scales are similar to hydrodynamics. However, MHD (Alfvén) waves can develop if a mean magnetic field is present. This can be a uniform dc magnetic field B_0 or a large local mean magnetic field. The waves introduce additional time scales, so that if the equations are linearized, MHD waves are associated with specific wave frequencies obtained from a dispersion relation. The interplay of waves and turbulent fluctuations (nonlinear activity) is actually a complex topic in MHD plasmas [7], pioneered by the works by Kraichnan [8]. Indeed, much of the subject of MHD turbulence is permeated by discussion of the balance of wavelike and nonlinear activity.

The range of frequencies of the waves is readily estimated. If a unit time is defined in terms of the largest length scale in the system (in a simulation, the $k=1$ mode) and the rms velocity, the nonlinear times extend from this unit time toward higher frequencies associated with the upper inertial range, and dissipative effects (at the end of the MHD scale description and the beginning of kinetic physics effects). MHD wave periods can be interspersed among those values, depending on the value of B_0. This may include incompressible Alfvén waves as well as magnetosonic (fast and slow)

*Present address: Departamento de Física, Facultad de Ciencias Exactas y Naturales, Universidad de Buenos Aires, Ciudad Universitaria, 1428, Buenos Aires, Argentina

waves if compressible effects are taken into account.

If the only time scales are the nonlinear and wave time scales, then one expects uncorrelated signals at frequencies lower than the lowest frequency wave or the reciprocal of the fundamental nonlinear time. This implies a flat frequency spectrum. At higher frequencies a different power law is expected. To generate low-frequency $1/f$ noise, it would appear necessary to generate signals correlated in time over much longer time scales than those that appear directly in the nonlinear dynamics, and for these signals to generate correlations over a range of time scales. One would expect these time scales which do not correspond directly to wave activity nor to the usual local nonlinear time, but instead involve very long time fluctuations of the fields.

If it appears, a f^{-1} spectral range contrasts with both the flat uncorrelated lowest frequencies, and the steeper spectrum that can be observed in the nonlinear time range or single peaks corresponding to the frequencies of the MHD waves. One possibility at higher frequencies is a $f^{-5/3}$ spectrum that could be explained, for example, by random sweeping [9] of the smaller fluctuations by the large eddies. Another possibility at higher frequencies is a f^{-2} power-law-type spectrum that would imply a single correlation time (defined in terms of the autocorrelation function) of the signal. A f^{-1} power-law spectrum means that there is no single correlation time in the signal.

A related antecedent of the results shown here is the observation of $1/f$ low-frequency noise in magnetic field fluctuations in the solar wind [10,11], which have so far remained not well understood. MHD simulations of the solar wind have attempted to show this type of fluctuation [12] but with negative results. Although the MHD system considered in this paper cannot be directly applicable to the solar wind plasma, it is interesting to show when $1/f$-type fluctuations appear in a basic situation as a step toward understanding the more complex observational results. There has been a suggestion of a $1/f$ signal in some dynamo simulations [6]. Below we find in particular that both MHD and hydrodynamics can, in some circumstances, show ranges of approximately $1/f$ spectral features at frequency much lower than the reciprocal large scale eddy turnover time. The longest wavelength modes of the driven system show this characteristic most clearly, and when these large scale modes make substantial contributions to the total energy budget, then one can see the $1/f$ signal in the single-point two-time correlations, and the Eulerian frequency spectrum. This leads us to the conclusion that fluid systems that admit an inverse cascade are most likely to generate $1/f$ noise.

II. EQUATIONS, NUMERICAL SIMULATIONS, AND DIAGNOSTICS

The compressible MHD equations (momentum and induction equations) in dimensionless units are

$$\frac{\partial \mathbf{v}}{\partial t} + \mathbf{v}\cdot\nabla\mathbf{v} = -\frac{1}{\rho\gamma M_s^2}\nabla p + \frac{\mathbf{j}\times\mathbf{B}}{\rho} + \frac{1}{R}\left(\nabla^2\mathbf{v} + \frac{1}{3}\nabla\nabla\cdot\mathbf{v}\right), \tag{1}$$

$$\frac{\partial \mathbf{b}}{\partial t} = \nabla\times(\mathbf{v}\times\mathbf{B}) + \frac{1}{R_m}\nabla^2\mathbf{b}, \tag{2}$$

where $\mathbf{v}$ is the plasma velocity, $\mathbf{B}=\mathbf{b}+\mathbf{B}_0$ is the magnetic field, with a fluctuating part $\mathbf{b}$ and a mean field (dc field) $\mathbf{B}_0$, $\mathbf{j}=\nabla\times\mathbf{b}$ is the current density, p is the pressure, and ρ is the plasma density. The units are based on a characteristic speed v_0, which for MHD is chosen to be the typical Alfvén speed of the magnetic field fluctuations, $v_0=v_a=\langle b^2\rangle^{1/2}/\sqrt{\rho_0}$ (with ρ_0 the initial density). The characteristic length scale is L, where the simulation box side length is defined as $2\pi L$. The unit time is $t_0=L/v_0$ which for MHD becomes the Alfvén crossing time. The dimensionless parameters appearing in the equations are the kinetic and magnetic Reynolds numbers $R=v_0L/\nu$, $R_m=v_0L/\mu$ (with ν the kinematic viscosity, μ the magnetic diffusivity) and the Mach number $M_s=v_a/c_s$, with c_s the sound speed.

The equations are complete with the continuity equation

$$\frac{\partial \rho}{\partial t} + \nabla\cdot(\rho\mathbf{v}) = 0, \tag{3}$$

and an equation of state, which here is the polytropic case, is assumed here,

$$\frac{p}{p_0} = \left(\frac{\rho}{\rho_0}\right)^{\gamma}, \tag{4}$$

where p_0 and ρ_0 are the initial pressure and density, and $\gamma=5/3$ (sound speed $c_s=\sqrt{\gamma p_0/\rho_0}$).

Equations (1) and (2) are solved with a triply periodic Fourier pseudospectral code. Results are reported here from runs with resolutions of 128^3 which allow several types of simulations (varying forcing parameters and mean magnetic field) and long time integrations, to obtain well-resolved frequency power spectra.

The Reynolds numbers are $R=R_m=400$. The scheme ensures exact energy conservation for the continuous time spatially discrete equations. The discrete time integration is done with a second-order Runge-Kutta method. The method ensures stabilized aliasing errors [13].

The initial state consists of nonzero fluctuation amplitudes for the velocity and magnetic field (in equipartition and with total mean squares normalized to 1) random phased in the k-space (wave-vector) shell $1\leq|\mathbf{k}|\leq 4$ (with k in units of $1/L$). Initial uniform density and a low Mach number $M_s=0.25$ are used. The initial cross helicity $H_c=\langle\mathbf{v}\cdot\mathbf{b}\rangle$ and magnetic helicity $H_m=\langle\mathbf{a}\cdot\mathbf{b}\rangle$ (with $\mathbf{a}$ the potential vector for the fluctuating magnetic field) are small.

Driving terms are added to Eqs. (1) and (2) to achieve a statistically steady state. This requires that we integrate the equation for hundreds or thousands of characteristic nonlinear times. The driving consists of independent vector forcing terms $\mathbf{f}_v$, $\mathbf{f}_b$ for the velocity and magnetic field evolution equations. The forcing is k dependent (only a range of modes are forced, with wave number between $k=1$ and $k=2$), with uncorrelated random intensities for each component at each time step and a memory function which implies a controlled correlation time of the driving. The forcing correlation time is set up to be of the order of the unit time (largest nonlinear

time). The uncorrelated random intensities of the forcing components assure no (statistical) injection of cross or magnetic helicity. This type of forcing represents a set of incoherent driven waves at a range of wave numbers. The absence of injection of cross or magnetic helicity is verified by checking the values of these quantities after a long time. In a typical run, for instance, the mean magnetic helicity is approximately 0.04, while the mean cross helicity is 0.006 (as compared with kinetic and magnetic energy, approximately 1). Temporary excursions of the magnetic helicity to positive or negative values of approximately 0.5 in some cases are however possible, a situation associated with the backtransfer phenomena discussed in Sec. VI.

Probes are set in the simulation box, to obtain time series of the fluctuating magnetic field or velocity field. Specifically a plane is chosen in the middle of the simulation box and a set of 64 probes in that plane, placed in a regular array of 8×8 points, is used to compute the extract data. A similar procedure was employed in [14] to study the presence of discrete modes within a turbulent system. A long time series of the single-point data are obtained (2000 unit times duration) to compute the frequency power spectra at the position of each probe. All spectra are computed from one Cartesian component of the fluctuations time series. For cases with a mean magnetic field, this component is perpendicular to the mean-field direction. Sampling rate of the time series is $\Delta t = 0.04$ unit times, which are 25 samples per unit time. The square absolute value of the fast Fourier transform of the time series is used to compute the power spectrum. An average spectrum is constructed using the spectra from each probe. This improves the statistics, reducing the noise, especially at high frequencies.

III. EULERIAN FREQUENCY SPECTRA IN HYDRODYNAMICS AND MAGNETOHYDRODYNAMICS

We carried out driven, dissipative spectral method simulations of hydrodynamics (HD), incompressible MHD (IMHD), and compressible MHD (CMHD). The Eulerian frequency spectra (Fourier transform of the two-time, single-point correlation function) were computed over very long times as described above. Figure 1 compares the results for the three cases. There is little or no suggestion of 1/f behavior in the HD case. The intriguing result for the two MHD cases is that, while there is no clearly identified 1/f range, there is more low-frequency power than in the HD run. The compensated spectra show a very gentle maximum well over a decade of frequency in a range corresponding to 0.1 or lower frequencies.

To further investigate the possibility that MHD can generate a 1/f signal, we examine next a series of compressible MHD runs with progressively stronger externally supported mean (dc) magnetic field $B_0=0,1,2,8$.

The frequency power spectra are shown in Fig. 2, for different values of $B_0=0,1,2,8$ from the top panel to the bottom panel. Several features can be observed in the frequency spectrum which extends for more than four orders of magnitude in frequency. The nonlinear time for the $k=1$ mode (unit time) corresponds to a frequency $f=1/(2\pi)$

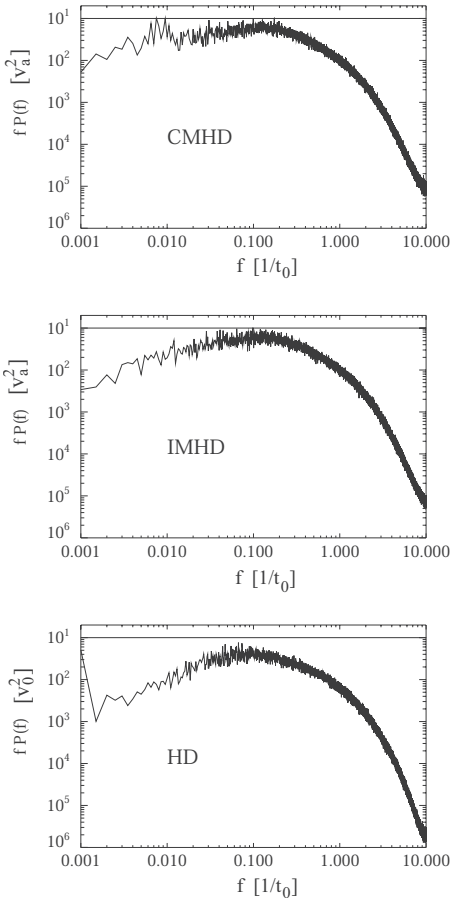

FIG. 1. Compensated frequency power spectrum $fP(f)$ (average over 64 probes) of magnetic field fluctuations for compressible MHD (CMHD, top panel), incompressible MHD (IMHD, middle panel), and velocity field fluctuations for incompressible hydrodynamics (HD, bottom panel). Units of V_a^2 and V_0^2 are used for the spectra $fP(f)$ and units of $1/t_0$ are used for frequency f, as defined in Sec. II.

≈ 0.16. The spectrum appears to be steep for higher frequencies, corresponding to nonlinear times for different k modes. Toward lower frequencies a 1/f power-law-type range is observed, and it is more prominent as the dc magnetic field increases. The panels show the compensated spectra $fP(f)$ to highlight the 1/f range (a constant value in the compensated spectrum). The range of 1/f fluctuations is between 2×10^{-3} to 2×10^{-1} for about two orders of magnitude. This is more clear for larger B_0, while it is not seen much for the $B_0=0$ case.

Another effect of the presence of a dc magnetic field $B_0\neq 0$ is the appearance of a broad peak in the spectra at around a frequency $f=B_0/(2\pi)$. This value is $f=0.16,0.32,1.27$ for $B_0=1,2,8$, respectively. This peak corresponds to an Alfvén wave with frequency $f=(kB_0)/(2\pi)$ for $k=1$. Other peaks appear in the $B_0=8$ frequency spectra, corresponding to compressive-type MHD waves, as well as higher wave-number (k) Alfvén waves.

The inset panels in Fig. 2 show the results of magnetic field fluctuations for a single probe during 500 unit times (a section of the full time series), for the different values of the

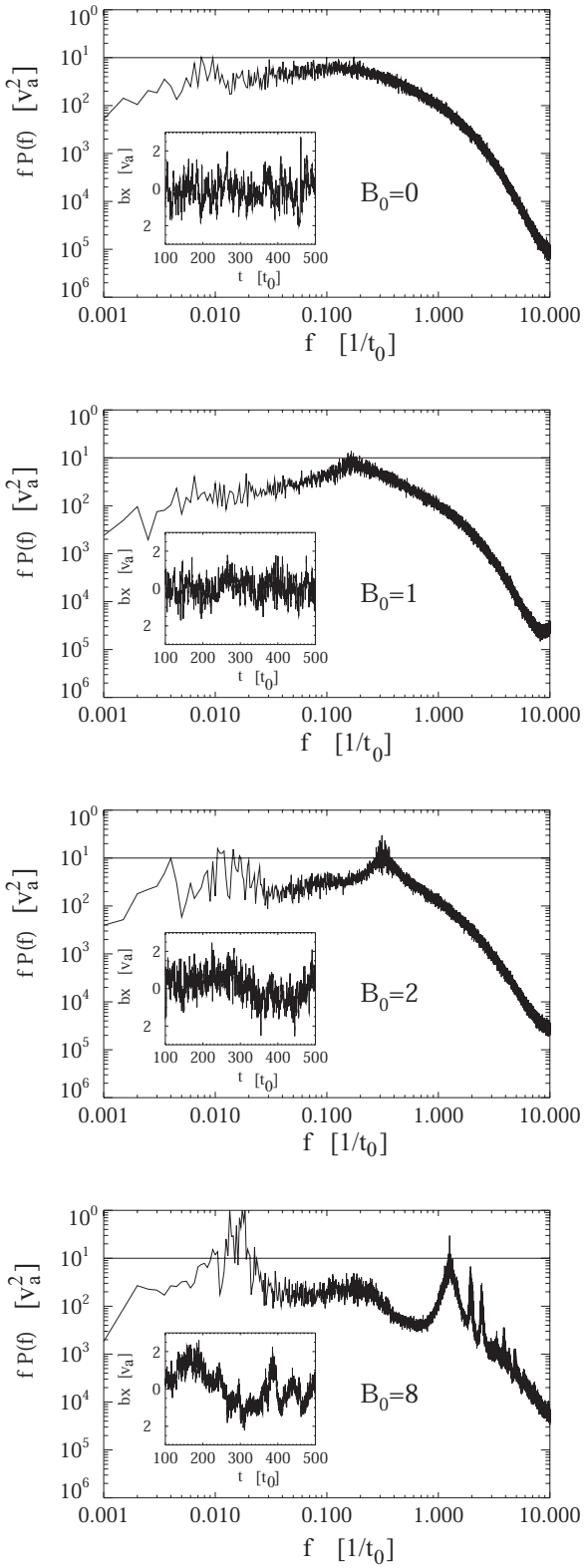

FIG. 2. Compensated frequency power spectrum $fP(f)$ (in units of V_a^2) of magnetic field fluctuations (averaged over 64 probes) for compressible MHD. Panels correspond to different values of the dc magnetic field $B_0=0,1,2,8$ (from top to bottom). Units of $1/t_0$ are used for frequency f. The inset panels show the magnetic field fluctuation (x component, in units of V_a) in a single probe in a selected period of time (in units of t_0).

TABLE I. Ratio of mean-square perpendicular magnetic field to mean-square total magnetic field and of mean-square fluctuating potential vector to mean-square magnetic field for different values of the dc field B_0, for compressible MHD runs.

	$B_0=0$	$B_0=1$	$B_0=2$	$B_0=8$
$\langle b_{2D}^2\rangle/\langle b^2\rangle$	0.34	0.39	0.59	0.94
$\langle a^2\rangle/\langle b^2\rangle$	0.48	0.38	0.55	0.87

dc magnetic field. It can be observed that as the dc magnetic field is increased there are longer time features observed in the time series, which correspond to low-frequency activity. The time features or oscillations observed are as long as 100 unit times, more clearly observed for the larger B_0 case. The noisy character of the spectra in the lowest decade of frequencies is due to the small number of samples of these fluctuations in the available time series. It is noted that the forcing correlation time is set up to be 1 unit time, so the observed features cannot be attributed to a direct result of the forcing.

Two additional diagnostics are made, to understand the properties of the observed low-frequency fluctuations. First, we want to quantify the well-known phenomenon of the development of *anisotropy* as the imposed magnetic field B_0 become stronger. As a measure of anisotropy, we computed the ratio of the two-dimensional mean-square magnetic field fluctuations and the total mean-square magnetic field fluctuations as a function of time, for different values of B_0. If $\mathbf{b}=\Sigma_{\mathbf{k}}e^{i\mathbf{k}\cdot\mathbf{r}}$, the two-dimensional part of the fluctuations is defined as $\mathbf{b}_{2D}=\Sigma_{\mathbf{k}\perp\mathbf{B}_0}e^{i\mathbf{k}\cdot\mathbf{r}}$, i.e., the sum of the modes with wave number perpendicular to the dc magnetic field. When there is no dc magnetic field, an arbitrary direction is chosen to compute the two-dimensional part. Table I shows the following results: as B_0 increases, the two-dimensional part becomes relatively larger, consistent with the well-known result of the development of anisotropy of MHD in the presence of a mean magnetic field [15–18].

Another useful diagnostic is the ratio of the mean-square vector potential (the fluctuating part) to the mean-square magnetic field fluctuation, as a function of time, for different values of B_0. The fluctuating vector potential is $\mathbf{a}$, such that $\mathbf{b}=\nabla\times\mathbf{a}$ (the mean field B_0 is not included in the computation). The mean value of $\mathbf{a}$ is excluded from the computation of $\langle a^2\rangle$, that is, if

$$\mathbf{a}=\sum_{\mathbf{k}}\mathbf{a}_{\mathbf{k}}e^{i\mathbf{k}\cdot\mathbf{r}}, \tag{5}$$

then $\langle a^2\rangle$ is defined as

$$\langle a^2\rangle=\sum_{\mathbf{k}\neq 0}|\mathbf{a}_{\mathbf{k}}|^2. \tag{6}$$

Since $|\mathbf{b}_{\mathbf{k}}|^2=k^2|\mathbf{a}_{\mathbf{k}}|^2$, then the ratio $\langle a^2\rangle/\langle b^2\rangle$ is a weighted mean of $1/k^2$. This ratio can be interpreted as a characteristic mean-square length scale. In theories of magnetic field line diffusion [19] it is sometimes called the "ultrascale" because it is independent of, and usually greater than, the correlation scale. In Table I we can see that this ratio gets bigger as B_0

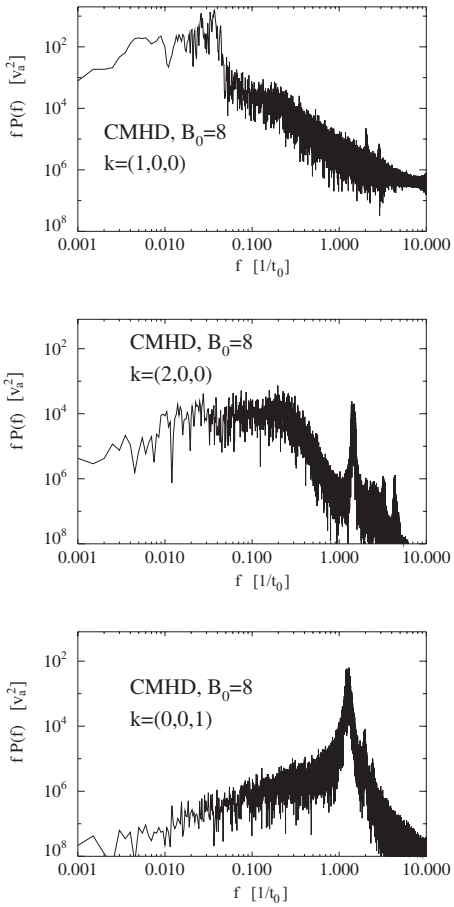

FIG. 3. Compensated frequency power spectrum for different **k** modes for $B_0=8$ (bottom panels). Units of V_a^2 are used for the spectra and units of $1/t_0$ are used for the frequency.

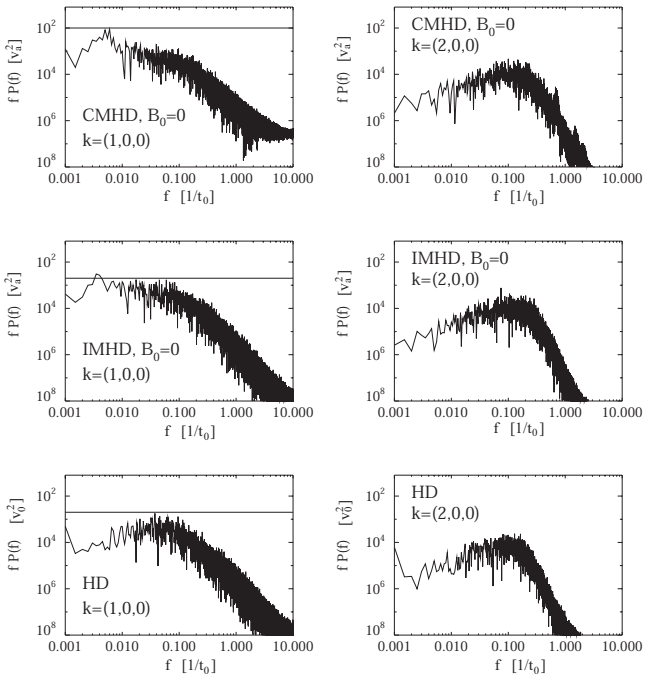

FIG. 4. Compensated frequency power spectrum for different **k** modes with $B_0=0$ for compressible MHD (top panels), incompressible MHD (middle panels), and velocity field modes for incompressible hydrodynamics (bottom panels). Units of V_a^2 and V_0^2 are used for the spectra and units of $1/t_0$ are used for the frequency.

increases. This shows that the lower k modes become dominant (in terms of power amplitude) as B_0 gets larger.

The above two diagnostics suggest that as anisotropy becomes more dominant, the steady MHD state becomes more dominated by the longest allowed wavelength. This provides important clues to explain the more robust appearance of a $1/f$ signal in the MHD cases with stronger B_0.

IV. FREQUENCY SPECTRA OF INDIVIDUAL MODES

There is a relationship between low-frequency activity (increased as B_0 increases) and the lowest allowable modes ($k=1$) in the system. To better assess this, a frequency power spectrum is computed for different single **k** modes. This is obtained from the time series of a mode $\mathbf{b}_\mathbf{k}(t)$, with the square absolute value of the fast Fourier transform of this time series. Results are shown in Figs. 3 and 4.

Figure 3 shows the compensated frequency power spectrum for modes $\mathbf{k}=(1,0,0)$, $\mathbf{k}=(0,0,1)$ and $\mathbf{k}=(2,0,0)$, where the three coordinates are x,y,z and the mean magnetic field is $\mathbf{B}_0=(0,0,B_0)$, with $B_0=8$. The spectrum for the transverse mode $\mathbf{k}=(1,0,0)$ shows a $1/f$ range, whereas this is not seen in the spectrum for the parallel mode $\mathbf{k}=(0,0,1)$ which shows instead a clear peak at the Alfvén frequency $f=kB_0/(2\pi)=1.27$. The $\mathbf{k}=(2,0,0)$ also shows some low-frequency activity but less clear than the $\mathbf{k}=(1,0,0)$ case. The results of the modes with $B_0=8$ are consistent with the probe-point frequency spectrum shown in Fig. 2 and the diagnostics discussed for Table I. Here, with large B_0, both two-dimensional activity and low k modes are dominant, and so the low-frequency activity is more clearly seen.

Figure 4 show results for $B_0=0$ and modes $\mathbf{k}=(1,0,0)$, $\mathbf{k}=(2,0,0)$ both in compressible MHD (top panels) and incompressible MHD (middle panels). Low-frequency activity with a $1/f$ range is seen for the $\mathbf{k}=(1,0,0)$ mode. The $\mathbf{k}=(2,0,0)$ mode shows instead less low-frequency power in the spectra. Unlike the probe-point frequency power spectrum shown in the top panel of Fig. 1 for the $B_0=0$ case, the mode frequency power spectra for the $k=1$ cases with $B_0=0$ shown in Fig. 4 have a low-frequency $1/f$ range. It seems then that the $1/f$ low-frequency content is directly related with the amount of power in the $k=1$ modes and, as was shown in Table I, this is less important for lower values of B_0.

The bottom panels of Fig. 4 show the single mode results for the HD case. There we can see that in neither $\mathbf{k}=(1,0,0)$ mode, nor in the $\mathbf{k}=(2,0,0)$ mode, is there any suggestion of $1/f$ activity.

An additional set of simulations were done with higher k forcing, $3<k_f<4$. No big differences are seen with respect to the previous cases, although less power is seen in low-frequency fluctuations for the $B_0=0$ case. This is consistent with the fact that less power exists in $k=1$ modes in comparison, due to the driving at higher k modes.

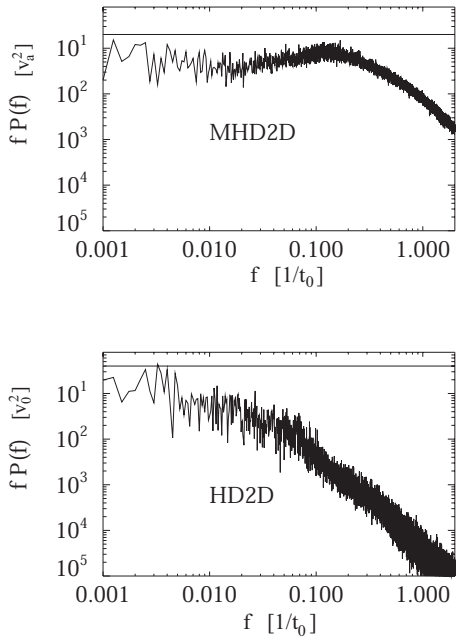

FIG. 5. Compensated frequency power spectrum $fP(f)$ (average over 64 probes) of: magnetic field fluctuations for two-dimensional incompressible MHD (MHD2D, top panel), and velocity field fluctuations for two-dimensional incompressible hydrodynamics (HD2D, bottom panel). Units of V_a^2 and V_0^2 are used for the spectra and units of $1/t_0$ are used for the frequency.

V. TWO-DIMENSIONAL MAGNETOHYDRODYNAMICS AND HYDRODYNAMICS RESULTS

A set of two-dimensional incompressible MHD and HD turbulence simulations was also performed. This means that the fluctuating magnetic field is $\mathbf{b}=(b_x(x,y),b_y(x,y))$ and the velocity field is $\mathbf{v}=[v_x(x,y),v_y(x,y)]$. No dc field was considered for these simulations.

A similar procedure as for the three-dimensional case discussed in the paper is followed, adding driving terms to the magnetic and velocity field equations and putting probes (in this case in the single plane of the simulations) to compute frequency spectra from the probes times series as well as frequency spectra of individual modes. Resolution of the runs is 128^2, Reynolds numbers are $R=R_m=400$ and the total time is 2000 eddy turnover times.

The Eulerian frequency spectra for the MHD and HD cases are shown in Fig. 5. There is a clear indication of a $1/f$ low-frequency range for both MHD and HD. This is in contrast to results in three dimensions which showed no clear hint of $1/f$ range for the hydrodynamic case.

The frequency spectra of individual modes are shown in Fig. 6. The top panels show the results for MHD for the x component of the lowest wave-number mode $\mathbf{k}=(0,1)$ and mode $\mathbf{k}=(0,2)$. [Note that the x component of mode $\mathbf{k}=(1,0)$ is 0 because of the incompressibility condition.] The bottom panels show the HD results. In both cases, MHD and HD, it is seen that the $1/f$ range is present in the $\mathbf{k}=(0,1)$ mode but is not observed (or less clear) in the $\mathbf{k}=(0,2)$ mode.

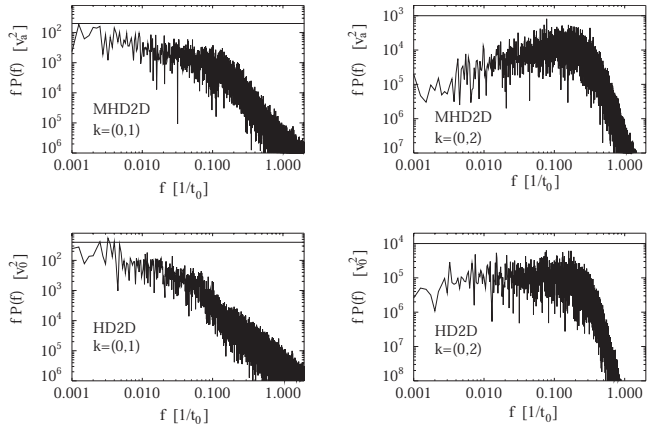

FIG. 6. Compensated frequency power spectrum for different **k** modes for MHD2D (top panels) and velocity field modes for HD2D (bottom panels). Units of V_a^2 and V_0^2 are used for the spectra and units of $1/t_0$ are used for the frequency.

VI. DISCUSSION AND CONCLUSIONS

These results indicate that the presence of $1/f$ low-frequency fluctuations in turbulence is directly related with the behavior of the lowest wave-number mode in the system. As an example of this, in three-dimensional MHD, when a strong background magnetic field exists, the familiar type of transverse spectral anisotropy is favored [15], and the system progressively two dimensionalizes. To the extent that this can occur, the mean-square vector potential discussed at the end of Sec. III asymptotically becomes an ideal quadratic invariant [20], and nonlinear couplings become less able to change the value of this quantity. Accordingly, the system must engage in stronger back transfer (or back scattering) of excitations toward lower wave number. Therefore, the lowest wave-number modes, with wave vectors perpendicular to the mean field, become dominant (see Table I), as we have seen in the computations, and a $1/f$ range of low-frequency fluctuations is clearly observed. Consistent with this interpretation, the $1/f$ signal is observed clearly in two-dimensional MHD where the addition of a second strictly conserved quadratic ideal invariant [20,21] ensures a genuine inverse cascade.

For MHD, when there is no background magnetic field, the existence of $1/f$ fluctuations is observed in the spectrum of the lowest wave-number mode, both in three and two dimensions. For hydrodynamics, the spectrum of the lowest wave number shows the existence of low-frequency fluctuations but no clear $1/f$ range in three dimensions. In contrast, two-dimensional hydrodynamics show a $1/f$ range in low-frequency fluctuations for the lowest wave-number mode.

A consistent interpretation of all of these results is that the $1/f$ range is associated mainly with the behavior of the longest wavelength modes, and seems to require the presence of, or the tendency toward, back transfer into those modes. Evidently, for three-dimensional (3D) hydrodynamics there is insufficient tendency toward two dimensionalization to enable the back-transfer effects that make possible a strong $1/f$ signal. However, inspecting Fig. 4, one cannot rule out a hint

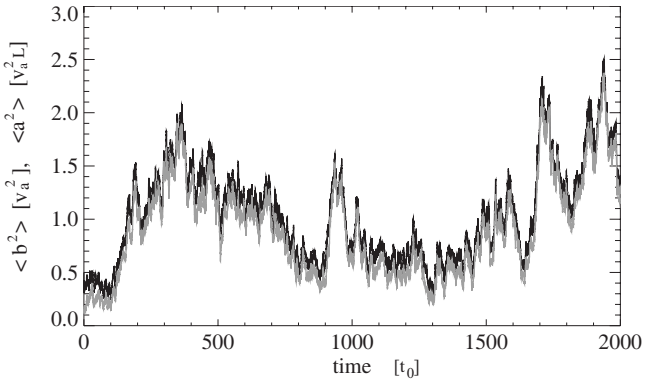

FIG. 7. Time history of fluctuation magnetic energy density $\langle b^2 \rangle$ (black) in units of V_a^2 and mean-square magnetic potential $\langle a^2 \rangle$ (gray) in units of $V_a^2 L$ (gray) for a driven 3D simulation with $B_0 = 8$. Units of t_0 are used for time.

of broadening of the peak in the 3D hydrodynamic $fP(f)$ spectrum of the $\mathbf{k}=(1,0,0)$ mode, compared, for example, with the relative sharpness of the turnover of the spectrum of the (2, 0, 0) mode in the same simulation.

When long time $1/f$ fluctuations are present in these simulations, they can have periods of $\tau \sim 10-100$ eddy turnover times [frequencies $f \sim 1/(2\pi\tau)$ between 0.001–0.01]. As an example of this we show in Fig. 7 time histories of the fluctuation energy and the mean-square magnetic potential from a 3D MHD simulation with strong mean magnetic field. The time range is 2000 units, corresponding to about 2000 eddy turnover times. It is clear that there is substantial structure in both quantities at time scales much larger than the nonlinear and wave time scales. Some of these excursions are quite large. These are the direct effect of the $1/f$ character. It is also notable that the variations of the two quantities are highly correlated at the scales visible in the figure, and that their ratio $\langle b^2 \rangle / \langle a^2 \rangle$ remains roughly in the range between 1 and 2. This indicates that most of the magnetic energy is in the longest wavelength modes. In this circumstance, for two-dimensional (2D) turbulence [20,21] the nonlinear part of the dynamics would be closely governed by conservation of energy and mean-square magnetic potential. In this 3D MHD case, which is highly anisotropic due to the strong mean magnetic field, it seems likely that in the presence of forcing, the "quasiconservation" of $\langle a^2 \rangle$ by subsequent spectral transfer may be intimately involved in the appearance of the $1/f$ behavior.

Consider, for example, the period shown in Fig. 7 prior to about $t=100$. The mean magnetic energy is about 0.4 in this period, and $\langle a^2 \rangle \approx 0.25$, so the mean magnetic wave number $\sqrt{\langle b^2 \rangle / \langle a^2 \rangle}$ is about 1.26. Later, between around $t=100$ and $t=350$, the energy rises to about 2.1 while $\langle a^2 \rangle$ rises to about 1.9, and the mean wave number is therefore reduced to about 1.05. Consequently the rise in energy is almost completely due to accumulation of excitation at the longest allowed wavelength. By further examining data such as these, one sees that the entire history of these quantities is dominated by the amount of energy in those modes. The conclusion is that the propensity of these modes to attract excitation supplied by the forcing, through back transfer and quasiconservation of the mean-square potential, and to accumulate it to a varying degree over long time scales, is responsible for the long time scale fluctuations that we see in this simulation. Note that there are excursions seen in the figure that have developed with time scales up to at least 100 time units. This appears to be the time domain signature of the spectral $1/f$ noise.

The picture above is that the low-frequency noise is associated with back transfer and the special role of the longest wavelength modes. It is worth recalling that these fluctuations cannot be attributed to the driving, since this is constructed so that its correlation time is of the order of 1 eddy turnover time ($f \sim 0.16$). Local nonlinear times $1/[kv(k)]$, based on the characteristic local length scale $1/k$ and velocity $v(k)$ are also of order 1 or smaller. Furthermore, all of the standard waves in these simulations are estimated to have frequencies >1 Hz. Therefore, the standard linear and the direct-cascade related nonlinear phenomena do not provide an explanation for the presence of the $1/f$ signal.

The key to further understanding the origin of these long time fluctuations must lie in the nature of the interaction of the lowest wave-number mode with much larger wave-number modes, say in the inertial range. Such couplings are highly nonlocal, in contrast to the standard Kolmogorov inertial range dynamical picture in which nonlinear interactions are dominated by couplings involving wave vectors that are either just lower than, or just greater than, the wave number in question. Here, singling out the longest wavelength mode of the system, it is clear that the dynamics cannot be local in the usual sense. In fact, we argue that, in nonlocal dynamics, the lowest wave-number mode $k=1$ interacts, through triads, with pairs of much larger wave-number modes. The time evolution of these interactions is controlled by the (comparative small) amplitude of the larger wave-number modes, but the large length scale (small k) of the lowest wave-number mode. This can be seen from the expression for this type of interaction which is of the (schematic) form

$$\frac{\partial b(k)}{\partial t} = -ik \sum_{k=p+q} v(q) b(p), \tag{7}$$

where $b(k)$, $v(q)$, $b(p)$ are generic Fourier mode amplitudes, with the constraint that $k=p+q$. In particular we consider the lowest wave-number mode $k=1$. If the particular interaction is local, then $k \sim p \sim q$ and the time scale of that interaction is given by $[kv(k=1)]^{-1} \sim 1$, whereas if the interaction is nonlocal, then $p,q \gg k=1$, $p \sim q$, and the time scale is $[kv(q)b(q)/b(k=1)]^{-1}$ which is much longer than the local time scale since $v(q)$, $b(q) \ll v(k=1)$, $b(k=1)$. This reasoning also suggests that for larger Reynolds numbers, as larger wave-number modes are available, the range of time scales involved in the nonlocal interaction with the $k=1$ mode becomes also larger, which means that presumably a larger range of $1/f$ would occur (provided the energy containing scales remain fixed).

The present results show the existence of low-frequency fluctuations in all of the simulations for the $k=1$ mode, con-

sistent with this view. However, the range of low-frequency fluctuations with $1/f$ spectra appears to be stronger for MHD (as well as two-dimensional hydrodynamics) as compared to three-dimensional hydrodynamics. Recent numerical simulations seem to support that energy transfer in MHD in the inertial range is still mostly local [22,23], although with more degree of nonlocality for the **v**-**b** couplings, especially in the case of forced MHD simulations. The lowest wave-number mode in MHD seems however to be involved in energy transfers with widely separated scales. An interesting example of this case was shown in a two-dimensional MHD numerical computation of the energy transfer between modes [24].

The coupling of the lowest wave-number mode with different wave-number modes can give rise to different characteristic times τ. A scale invariant distribution of characteristic times $G(\tau) \sim 1/\tau$ is needed [2,3] in order to obtain the $1/f$ range in the frequency spectrum. Although nonlocal energy transfer can give in our view an explanation of the broad distribution of characteristic times observed here, the origin of the precise invariant form of this distribution of times remains unclear to us.

We note that the dynamics of the longest allowed wavelength modes may have a widespread tendency to display $1/f$ frequency spectra, according to the above scenario. The associated clearly defined $1/f$ Eulerian frequency spectra requires a much stronger condition, since this spectrum involves the total contribution to the time variation due to all Fourier modes of the system. The significance of the present study is that we have seen that cases in which the Eulerian spectrum shows a $1/f$ character are precisely those cases in which inverse cascade (or, back transfer) cause the longest wavelength mode to become energetically significant in the global energy budget. Then its characteristic temporal signal, which is $1/f$ in nature, becomes detectable in the low-frequency spectral characteristics of the system as a whole. This may be viewed as a form of self-organization in the time domain. It remains to see if this view remains viable in examining additional dynamical systems of this type in which special modes are singled out by the turbulent dynamics.

This research was supported by NASA Contracts Nos. NNG06GD47G and NNG04GA54G, and NSF Grant No. ATM-0539995. PD is a member of the Carrera del Investigador Científico of CONICET.

[1] $P(f)=(2\pi)^{-1}\int R(t)e^{-2\pi ift}dt$, for time lag t, and autocorrelation $R(t)=\langle b(0)b(t)\rangle$ defined in terms of an appropriate average $\langle\cdots\rangle$, with $b(t)$ as the fluctuating field.
[2] S. Machlup, *Sixth International Conference on Noise in Physical Systems* (National Bureau of Standards, Washington, DC, 1981), p. 157.
[3] A. VanderZiel, Physica **16**, 359 (1950).
[4] E. W. Montroll and M. F. Shlesinger, Proc. Natl. Acad. Sci. U.S.A. **79**, 3380 (1982).
[5] P. Bak, C. Tang, and K. Wiesenfeld, Phys. Rev. A **38**, 364 (1988).
[6] Y. Ponty, H. Politano, and J.-F. Pinton, Phys. Rev. Lett. **92**, 144503 (2004).
[7] Y. Zhou, W. H. Matthaeus, and P. Dmitruk, Rev. Mod. Phys. **76**, 1015 (2004).
[8] R. H. Kraichnan Phys. Fluids **8**, 1385 (1965).
[9] S. Chen and R. H. Kraichnan, Phys. Fluids A **1**, 2019 (1989).
[10] W. H. Matthaeus and M. L. Goldstein, Phys. Rev. Lett. **57**, 495 (1986).
[11] W. H. Matthaeus, B. Breech, P. Dmitruk, A. Bemporad, G. Poletto, M. Velli, and M. Romoli, Astrophys. J. **657**, L121 (2007).
[12] L. Ofman, J. Geophys. Res. **109**, A07102 (2004).
[13] S. Ghosh, M. Hossain, and W. H. Matthaeus, Comput. Phys. Commun. **74**, 18 (1993).
[14] P. Dmitruk, W. H. Matthaeus, and L. Lanzerotti, Geophys. Res. Lett. **31**, L21805 (2004).
[15] J. Shebalin, W. H. Matthaeus, and D. C. Montgomery, J. Plasma Phys. **29**, 525 (1983).
[16] S. Oughton, W. H. Matthaeus, and E. R. Priest, J. Fluid Mech. **280**, 95 (1994).
[17] W. C. Muller, D. Biskamp, and R. Grappin, Phys. Rev. E **67**, 066302 (2003).
[18] W. C. Muller and R. Grappin, Phys. Rev. Lett. **95**, 114502 (2005).
[19] W. H. Matthaeus, P. C. Gray, D. H. Pontius, and J. W. Bieber, Phys. Rev. Lett. **75**, 2136 (1995).
[20] D. Fyfe and D. Montgomery, J. Plasma Phys. **16**, 181 (1976).
[21] D. Fyfe, D. Montgomery, and G. Joyce, J. Plasma Phys. **17**, 369 (1977).
[22] O. Debliquy, M. K. Verma, and D. Carati, Phys. Plasmas **12**, 042309 (2005).
[23] A. Alexakis, P. D. Mininni, and A. Pouquet, Phys. Rev. E **72**, 046301 (2005).
[24] G. Dar, M. K. Verma, and V. Eswaran, Physica D **157**, 207 (2001).